JACS
JOURNAL OF THE AMERICAN CHEMICAL SOCIETY
pubs.acs.org/JACS
Article

Chain-End Controlled Depolymerization Selectivity in α,α-Disubstituted Propionate PHAs with Dual Closed-Loop Recycling and Record-High Melting Temperature

Li Zhou, Zhen Zhang, Ainara Sangroniz, Changxia Shi, Ravikumar R. Gowda, Miriam Scoti, Deepak K. Barange, Clarissa Lincoln, Gregg T. Beckham, and Eugene Y.-X. Chen*

Cite This: J. Am. Chem. Soc. 2024, 146, 29895−29904
Read Online

ABSTRACT: Within the large poly(3-hydroxyalkanoate) (PHA) family, C3 propionates are much less studied than C4 butyrates, with the exception of α,α-disubstituted propionate PHAs, particularly poly(3-hydroxy-2,2-dimethylpropionate), P3H(Me)$_2$P, due to its high melting temperature (T_m ~ 230 °C) and crystallinity (~76%). However, inefficient synthetic routes to its monomer 2,2-dimethylpropiolactone [(Me)$_2$PL] and extreme brittleness of P3H(Me)$_2$P largely hinder its broad applications. Here, we introduce simple, efficient step-growth polycondensation (SGP) of a hydroxyacid or methyl ester to afford P3H(Me)$_2$P with low to medium molar mass, which is then utilized to produce lactones through base-catalyzed depolymerization. The ring-opening polymerization (ROP) of the 4-membered lactone leads to high-molar-mass P3H(Me)$_2$P, which can be depolymerized by hydrolysis to the hydroxyacid in 99% yield or methanolysis to the hydroxyester in 91% yield, achieving closed-loop recycling via both SGP and ROP routes. Intriguingly, the chain end of the SGP-P3H(Me)$_2$P determines the depolymerization selectivity toward 4- or 12-membered lactone formation, while both can be repolymerized back to P3H(Me)$_2$P. Through the formation of copolymers P3H(Me/R)$_2$P (*R* = Et, ^{n}Pr), PHAs with high tensile strength and ductility, coupled with high barriers to water vapor and oxygen, have been created. Notably, the PHA structure−property study led to P3H(^{n}Pr)$_2$P with a record-high T_m of 266 °C within the PHA family.

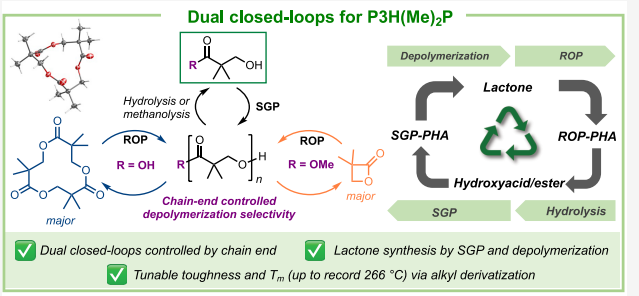

INTRODUCTION

Poly(3-hydroxyalkanoate)s (PHAs), a family of aliphatic polyesters, are naturally accumulated via biological processes[1−11] or chemically synthesized using molecular catalysis.[12−16] Among them, a C4 butyrate PHA, poly(3-hydroxybutyrate) (P3HB), attracts the most attention, but its lack of melt processability, mechanical brittleness, and unrealized chemical recyclability has limited its broader application. To address these issues, many studies have put forward innovative solutions.[17−24] Notably, Coates et al. chemically synthesized a nature-inspired poly(3-hydroxy-2-methylbutyrate) (PHMB)[25] by ring-opening polymerization (ROP) of 4-membered lactones derived from 2-butene and CO, and also uncovered tacticity-independent crystallinity and excellent mechanical properties of PHMB.[26,27] Coincidently, we reported that α,α-dimethylated P3HB, poly(3-hydroxy-2,2-dimethylbutyrate) [P3H(Me)$_2$B], also exhibits tacticity-independent crystallinity and thus is always semicrystalline, regardless of its tacticity.[28,29] Importantly, it is mechanically tough, melt-processable, and chemically recyclable; it can be readily scaled up to hundreds of grams with a solvent-free polymerization using a commercial organic catalyst.[28] Recognizing step-growth polycondensation (SGP) that is commonly practiced in the production of industrial polymers,[30,31] we previously attempted SGP of a hydroxyacid (HA), 3-hydroxy-2,2-dimethylbutyric acid, to produce P3H(Me)$_2$B, but it primarily yielded oligomers (8−9 repeating units).[28] This limitation arises due to the secondary alcohol in the HA monomer of butyrate PHA, which impedes the efficiency of polycondensation.

In comparison, C3 propionate PHAs are much less studied, except for α,α-disubstituted propionate PHAs, particularly poly(3-hydroxy-2,2-dimethylpropionate), P3H(Me)$_2$P, which has been studied since 1970s to reveal a higher melting-transition temperature (T_m = 220−230 °C) than the parent poly(3-hydroxypropionate) (P3HP, T_m = 70−80 °C) and even isotactic (*it*-) P3HB (T_m = 170−180 °C).[32−34] Moreover, a more impressive feature of the P3H(Me)$_2$P prepared in this work and crystallized from the melt is its high degree of

Received: August 29, 2024
Revised: October 1, 2024
Accepted: October 1, 2024
Published: October 16, 2024

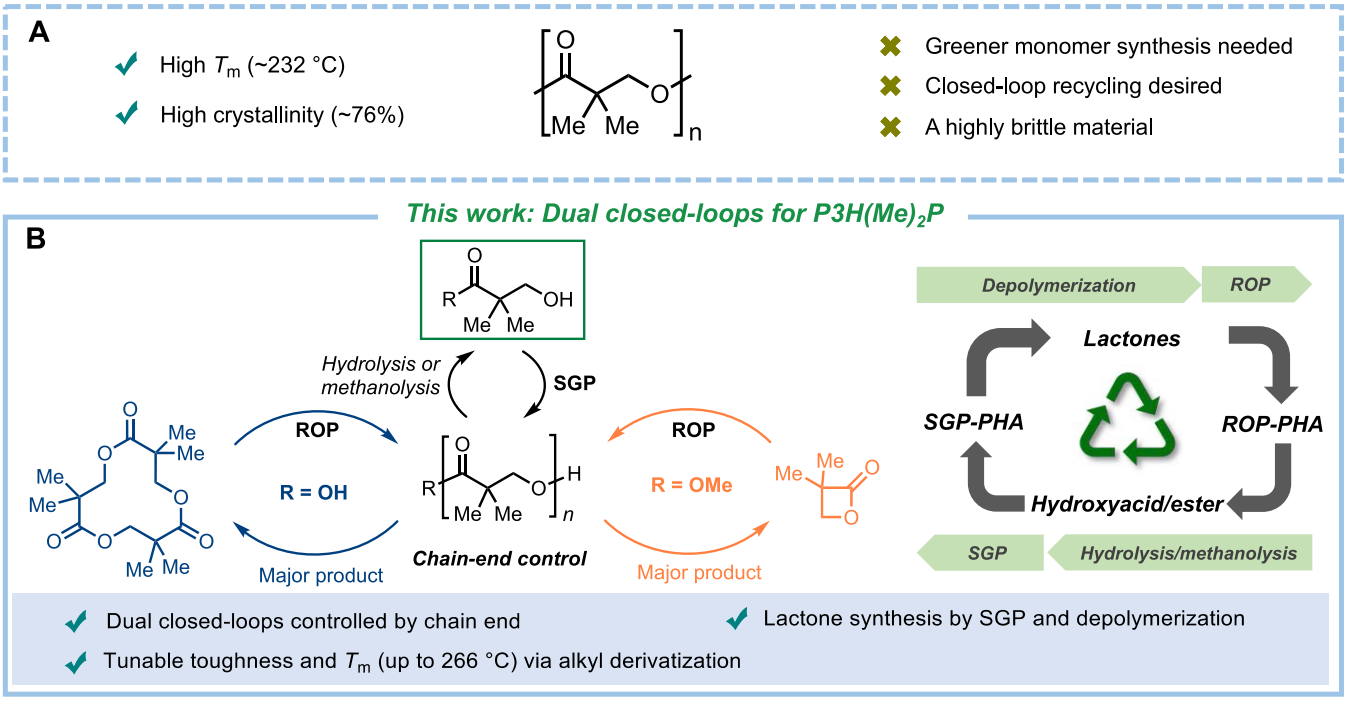

Figure 1. A summary of properties and challenges of P3H(Me)$_2$P, and key achievements of this work. (A) Favorable thermal properties (high T_m and crystallinity) and three unmet challenges facing P3H(Me)$_2$P. (B) This work (i) achieved chemical circularity through dual SGP and ROP closed-loops; (ii) found unique chain-end controlled depolymerization selectivity; (iii) solved brittleness via copolymer formation; and (iv) discovered a PHA, P3H(^{n}Pr)$_2$P, with a record-high T_m.

crystallinity (~76%), which is comparable to that of linear polyolefins crystallized at high crystallization temperature.[35−37] This observation indicates efficient crystallization and a high regularity of the structure. Base-catalyzed depolymerization of P3H(Me)$_2$P (obtained by the ROP) was reported in a 2-page patent,[38] but no information on the polymer used and characterizations of the resulting condensed product (which was assumed to be pivalolactone or 2,2-dimethylpropiolactone (Me)$_2$PL) was disclosed. Pyrolysis of P3H(Me)$_2$P was investigated extensively by mass spectroscopy, revealing formation of a distribution of cyclic oligomers.[39−43] Thermal degradation of P3H(Me)$_2$P having pivalate and carboxylate chain ends was interrogated by two independent mechanisms, reverse polymerization[44] and random chain scission degradation.[45] Cyclooligomerization of pivalolactone in dilute solution with alkali metal alkoxides is also a suitable strategy for the synthesis of macrocyclic oligomers as a mixture, from which the tetramer was isolated and structurally characterized.[46] The structure of the trimer or triolide, [(Me)$_2$PL]$_3$, obtained in 8% yield from cyclization of a hydroxy diester, was also reported.[47] However, the current P3H(Me)$_2$P also faces three challenges to broaden its commercial implementation and application (Figure 1A). First, it is primarily synthesized from ROP of (Me)$_2$PL.[28,32] The preparation of (Me)$_2$PL typically involves the use of hazardous and difficult-to-handle or explosive reagents such as ketenes.[48] In this context, a better method involving regioselective carbonylation of isobutylene oxide was developed by Coates et al.[49,50] Second, P3H(Me)$_2$P is a brittle material and lacks the ductility typically required for many applications. Third, toward achieving a circular plastics economy,[51−57] it would be desirable to demonstrate closed-loop chemical recycling of P3H(Me)$_2$P.

To address the above known issues (Figure 1A) associated with P3H(Me)$_2$P, we hypothesized that developing an efficient SGP route to access P3H(Me)$_2$P, with even low to medium molar mass, coupled with its selective depolymerization to the lactone for high-molar-mass PHA production, could effectively solve the above problems. First, the HA monomer for SGP, 3-hydroxypivalic acid or formally 3-hydroxy-2,2-dimethylpropionic acid [3H(Me)$_2$PA], is readily (commercially) available and contains the reactive primary alcohol and, additionally, this α,α-dimethylated PHA is devoid of α-protons, thus suppressing potential side reactions such as dehydration and *cis*-elimination at high SGP temperatures. Worth noting here is that SGP is not effective in PHA synthesis involving HAs bearing secondary alcohols, as the polymerization is terminated by a series of side reactions.[58,59] Second, the resulting SGP-P3H(Me)$_2$P should be hydrolytically depolymerized back to the HA or depolymerized via base catalysis to the lactone, either 4-membered (Me)$_2$PL or potentially 12-membered [(Me)$_2$PL]$_3$, depending on the chain end of the PHA, thereby closing both SGP and ROP loops in chemical recycling (Figure 1B). A potential challenge in closing the ROP loop via [(Me)$_2$PL]$_3$ is the low reactivity of this medium-size lactone, as the trimeric β-butyrolactone ([β-BL]$_3$) obtained from the depolymerization of P3HB can only be repolymerized to oligomers with a low molar mass (M_n ~ 5 kDa).[60,61] We showed in this work that, remarkably, the ROP of recycled (Me)$_2$PL afforded high absolute weight-average-molar-mass (M_w = 232 kDa) PHA, and even the recycled [(Me)$_2$PL]$_3$ can be repolymerized to obtain P3H(Me)$_2$P with M_w up to 71.4 kDa (*vide infra*). Third, through copolymerization to incorporate repeating units with Me/Et or Me/^{n}Pr substituents, thermal and mechanical properties of the resulting PHA copolymers could be readily tailored to potentially achieve balanced performance properties. Guided by the above three hypotheses, this work is focused on P3H(Me)$_2$P and its alkyl derivatives, aiming to solve these three key challenges.

https://doi.org/10.1021/jacs.4c11920
J. Am. Chem. Soc. 2024, 146, 29895−29904

RESULTS AND DISCUSSION

SGP Route to P3H(Me)$_2$P. SGP has long been a favored polymerization method to produce polyesters, especially those [A_2 + B_2]-type, high-melting polymers such as poly(ethylene terephthalate) (PET), due to its simplicity and cost-effectiveness. However, PHA synthesis using SGP of AB-type HAs containing a secondary alcohol to produce PHAs bearing acidic α-protons (α to the carbonyl), which hinder the reactivity of the HAs and promote dehydration of the HAs and PHAs at high temperatures, is largely ineffective. In this context, the SGP route to the high-T_m P3H(Me)$_2$P with appreciable molar mass appears especially attractive and feasible, as its corresponding AB monomer, 3H(Me)$_2$PA, contains the more reactive primary alcohol and, additionally, the PHA is devoid of α-protons. The α,α-dimethyl substitution in P3H(Me)$_2$P also synergistically suppress *cis*-elimination, thereby enhancing the PHA thermal stability.[28]

Accordingly, we investigated the SGP of 3H(Me)$_2$PA and its methyl ester, methyl 3-hydroxy-2,2-dimethylpropanoate (M3H-(Me)$_2$P), in the presence of catalysts such as Ti(O^{n}Bu)$_4$ and B(C_6F_5)$_3$ typically employed for SGP processes. As summarized in Table 1, the efficient synthesis of P3H(Me)$_2$P has been

Table 1. Results of SGP of 3H(Me)$_2$PA and M3H(Me)$_2$P[a]

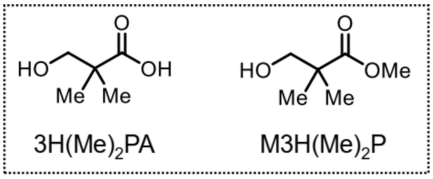

run	monomer	catalyst	yield (%)[b]	M_w[c] (kDa)	$Đ$[c] (M_w/M_n)
1	3H(Me)$_2$PA	Ti(O^{n}Bu)$_4$	92	26.4	2.26
2	3H(Me)$_2$PA	B(C_6F_5)$_3$	87	29.1	1.39
3[d]	3H(Me)$_2$PA	Ti(O^{n}Bu)$_4$	63	34.2	1.50
4	M3H(Me)$_2$P	Ti(O^{n}Bu)$_4$	95	17.7	1.72

[a]Conditions: monomer (30 mmol), [monomer]/[catalyst] ([M]/[Cat]) = 100/1. [b]Isolated yield. [c]Weight-average molar mass (M_w) and dispersity ($Đ$ = M_w/M_n) determined by size exclusion chromatography (SEC) at 40 °C in hexafluoroisopropanol (HFIP, $(CF_3)_2$CHOH) coupled with a Wyatt Technology miniDAWN TREOS multiangle light scattering detector and a Wyatt Technology Optilab T-rEX differential refractometer for absolute M_w. [d][M]/[Cat] = 1000/1.

achieved, thanks to the structures of the HA and P3H(Me)$_2$P that mitigate crotonate end-group formation through trans-esterification and elimination/termination due to the absence of α-hydrogens, the two types of side reactions commonly encountered in the previous PHA synthesis via SGP. More specifically, the SGP of 3H(Me)$_2$PA and M3H(Me)$_2$P, when catalyzed by Ti(O^{n}Bu)$_4$ or B(C_6F_5)$_3$, afforded P3H(Me)$_2$P with M_w ranging from 17.7 to 34.2 kDa. This SGP process is readily scalable, as shown by a 666-g laboratory scale that produced P3H(Me)$_2$P with a comparable molar mass and no alkene end groups revealed by ^{1}H NMR spectra (Figures S1 and S2). Noteworthy is that similar thermal properties are observed for the P3H(Me)$_2$P materials produced by SGP and ROP routes (*vide infra*), underscoring the practical usability of the SGP-produced P3H(Me)$_2$P.

Chain-End Controlled Depolymerization Selectivity. On the basis of the *gem*-disubstitution Thorpe−Ingold effect, which has been shown to promote ring closure from the ring-opened form by stabilizing the strained rings,[62−66] we envisioned a synergistic benefit of α,α-dimethyl substitution in P3H(Me)$_2$P, which not only enhances thermal stability (*vide supra*) but also renders chemical recyclability by direct depolymerization to the lactone monomer. In our initial experiments (Figure 2, Table S1), a P3H(Me)$_2$P sample, synthesized via SGP of 3H(Me)$_2$PA, was subjected to depolymerization conditions (5 wt % NaOH, 250 °C, ∼ 200 mTorr) using a sublimation setup, affording solid products in ∼90% yield. Through recrystallization, the pure product (53% yield) was identified by NMR (Figure S3), LCMS (Figure S4), and single-crystal X-ray diffraction analyses (Figure 2) to be the 12-membered trimeric lactone [(Me)$_2$PL]$_3$[47] (Table S1, Run 1), while other compounds in the crude solid product mixture contained various oligomers. Notably, when NaOMe was utilized instead of NaOH, the [(Me)$_2$PL]$_3$ content increased to 70%. Additionally, using a distillation setup recovered the 4-membered lactone (Me)$_2$PL in 9% yield. This depolymerization process was again performed on a 3.9-g scale, affording 2.6 g of pure [(Me)$_2$PL]$_3$ in 66% isolated yield after recrystallization (Table S1, Run 3).

More interestingly, when a P3H(Me)$_2$P sample obtained from SGP of methyl ester M3H(Me)$_2$P was subjected to depolymerization conditions (5 wt % NaOH, 230 °C, ∼ 0.2 Torr), the recovered pure product is monomeric lactone (Me)$_2$PL in 53% isolated yield (Table S1, Run 5). The use of NaOMe mixed with the same P3H(Me)$_2$P also resulted in pure (Me)$_2$PL in 58% isolated yield (Table S1, Run 6, and Figure S5). Additional depolymerization runs consistently produced both (Me)$_2$PL (52% isolated yield) and [(Me)$_2$PL]$_3$ (35% isolated yield) (Table S1, Run 8). Notably, the distillation setup can completely separate these two lactones: the low-boiling liquid (Me)$_2$PL is condensed in the receiving flask at the end, but the solid [(Me)$_2$PL]$_3$ is precipitated as crystals on the distillation head.

The above disparate product outcomes observed in the base-catalyzed depolymerization of P3H(Me)$_2$P with different chain ends (which are predetermined by the monomer source, HA vs its ester), prompted us to rationalize mechanistic scenarios outlined in Figure 3 that can explain these intriguing findings. It is noted first that both chain ends in P3H(Me)$_2$P-CO_2H (with the carboxylic acid and hydroxyl chain ends), derived from the SGP of the HA 3H(Me)$_2$PA, can initiate the depolymerization process, albeit with a significantly faster initiation rate for a carboxylate anion (Figure 3, rate (route 2) > rate (route 3 or 4)). This distinction is evident in the shorter depolymerization time of P3H(Me)$_2$P-CO_2H compared to that of P3H(Me)$_2$P-CO_2Me (with the methyl ester chain end), derived from the SGP of M3H(Me)$_2$P. Second, the depolymerization of P3H-(Me)$_2$P-CO_2H exhibits two distinct pathways. One pathway involves backbiting of the carboxylate to form (Me)$_2$PL (Figure 3, route 1) or its trimer (Figure 3, route 2). However, due to the challenges associated with the carboxylate anion attacking the C−O bond through SN_2 and the high ring strain of (Me)$_2$PL, generating (Me)$_2$PL under this path would be more difficult. Consequently, the main product is the more thermally stable [(Me)$_2$PL]$_3$. The second pathway involves a decarboxylation reaction (Figure 3, route 5), which can occur under high temperature and base conditions, leading to the formation of isobutylene—a byproduct (Figure S6) alongside (Me)$_2$PL and [(Me)$_2$PL]$_3$. Third, the utilization of P3H(Me)$_2$P-CO_2Me, which lacks the carboxylic acid chain end, effectively mitigates

https://doi.org/10.1021/jacs.4c11920
J. Am. Chem. Soc. 2024, 146, 29895−29904

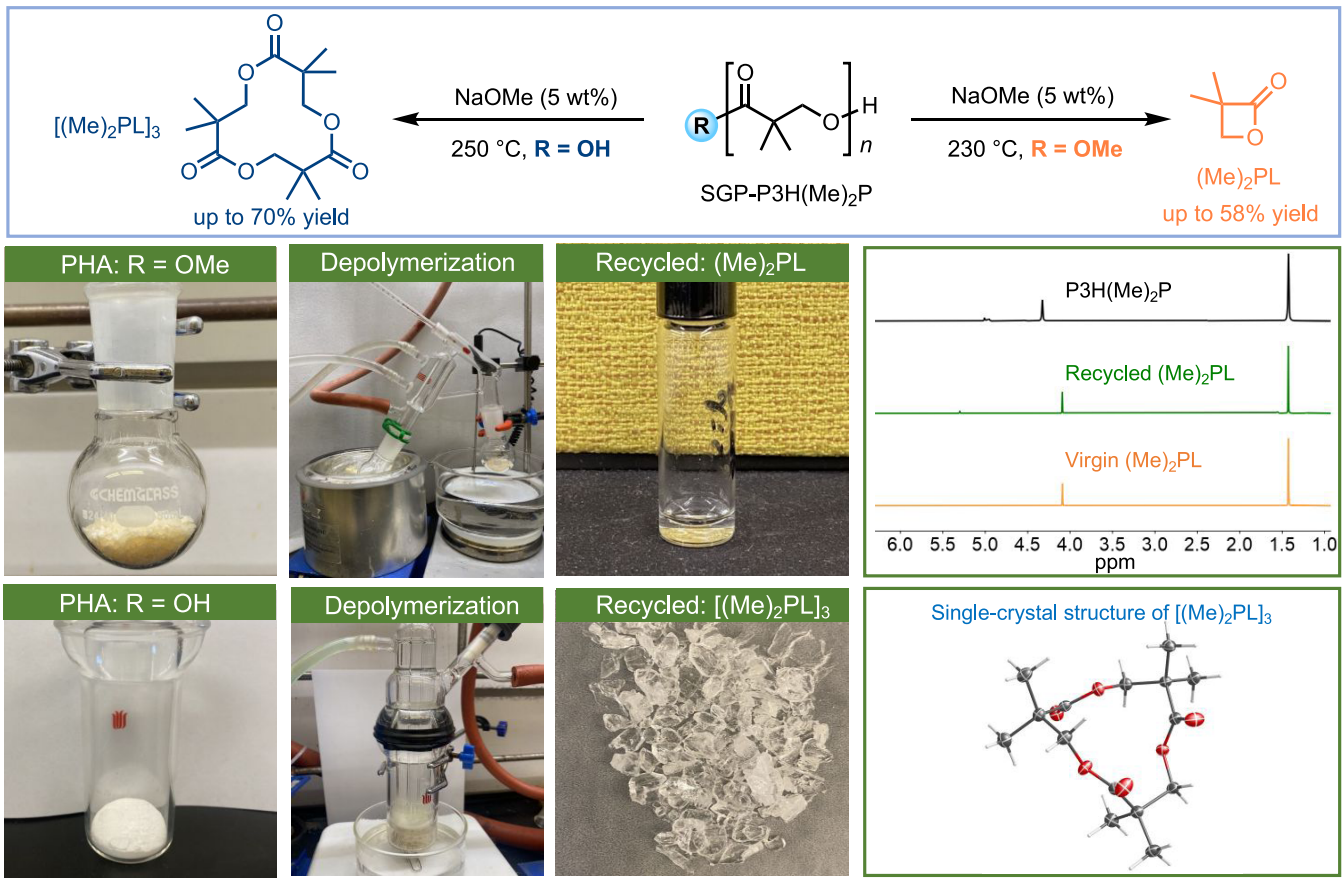

Figure 2. Production of 4- and 12-membered lactones (for ROP to PHA with higher molar mass) through chain-end controlled, base-catalyzed depolymerization of P3H(Me)$_2$P prepared by SGP. Top row: schematic synthetic pathways; middle row: photos of the reaction setup, physical state of starting P3H(Me)$_2$P (solid) and (Me)$_2$PL (liquid), and stacked NMR spectra of the starting PHA, recycled (Me)$_2$PL, and virgin (Me)$_2$PL; bottom row: photos of the reaction setup, physical state of starting P3H(Me)$_2$P (powder) and [(Me)$_2$PL]$_3$ (crystalline solid), and single-crystal X-ray structure of [(Me)$_2$PL]$_3$ formed via base-catalyzed depolymerization.

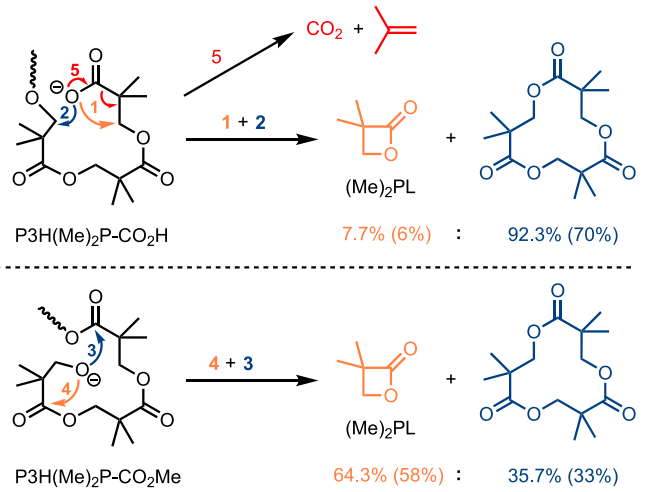

Figure 3. Proposed pathways to different products for base-catalyzed depolymerization of P3H(Me)$_2$P with different chain ends. For the sake of clarity, the anionic forms of the carboxylic acid and hydroxyl chain ends are invoked here under base catalysis. The isolated yields are indicated in parentheses.

the formation of isobutylene, making the depolymerization process initiated by the alkoxy chain end the predominant pathway. This alkoxy-initiated pathway also generates (Me)$_2$PL and its trimer (Figure 3, routes 3 and 4). Importantly, the higher propensity of the alkoxy to attack the ester carbonyl, forming the lactone, makes the ring closure to (Me)$_2$PL more favorable compared to the depolymerization process of the PHA with the carboxylate (route 4 is much more favorable than route 1). Hence, the PHA with the ester chain end significantly improves its depolymerization selectivity toward the formation of the desired (Me)$_2$PL. The preorganized geometries depicted on the left column of Figure 3 imply a much higher energy pathway for the unobserved dimeric (8-membered) lactone.

Dual ROP and SGP Closed-Loop Recycling of P3H(Me)$_2$P. As described above, the base-catalyzed bulk depolymerization of P3H(Me)$_2$P afforded the monomeric 4-membered lactone (Me)$_2$PL or trimeric 12-membered lactone [(Me)$_2$PL]$_3$ as the major product, depending on the PHA chain ends. Subsequently, we investigated the ROP of these lactones in detail, aiming to close the chemical recycling loop via ROP. We noted here that, besides the above depolymerization pathway to produce (Me)$_2$PL, it can also be obtained through a straightforward one-step lactonization of commercially available 3H(Me)$_2$PA or 3-chloropivalic acid in 63−93% yields (see Supporting Information). This lactonization method was also extended to the synthesis of other alkyl-substituted 4-membered lactone derivatives (*R*)$_2$PL (*R* = Et, ^{n}Pr, ^{n}Bu).

At the outset, the ROP of (Me)$_2$PL was explored by employing different organic base catalysts and reaction conditions (Table 2). Given the insolubility of highly crystalline P3H(Me)$_2$P in common organic solvents, the ROP was carried

https://doi.org/10.1021/jacs.4c11920
J. Am. Chem. Soc. 2024, 146, 29895−29904

Table 2. Selective Results for the ROP of $(Me)_2PL$ and $[(Me)_2PL]_3$[a]

run	monomer	catalyst	[M]/[Cat]/[I]	temp. (°C)	time (h)	conversion (%)[b]	M_w[c] (kDa)	M_n[c] (kDa)	$Đ$[c] (M_w/M_n)
1	$(Me)_2PL$	TBD	400/1/1	70	1	98	20.6	17.6	1.17
2	$(Me)_2PL$	TBD	3200/1/1	70	1	62	64.7	42.1	1.54
3	$(Me)_2PL$	DBU	1600/1/1	70	1	90	74.1	47.8	1.55
4	$(Me)_2PL$	DBU	3200/1/1	70	1	58	110	65.5	1.67
5	$(Me)_2PL$	^{t}Bu-P_4	400/1/1	70	1	100	23.0	20.7	1.11
6	$(Me)_2PL$	^{t}Bu-P_4	1600/1/1	70	1	100	86.7	58.7	1.48
7	$(Me)_2PL$	^{t}Bu-P_4	6400/1/1	70	1	100	232	162	1.43
8	$[(Me)_2PL]_3$	^{t}Bu-P_4	100/1/1	120	12	100	31.2	10.5	2.97
9	$[(Me)_2PL]_3$	$La(OBn)_3$	200/1	120	12	75	21.5	12.2	1.77
10	$[(Me)_2PL]_3$	$La(OBn)_3$	800/1	120	12	62	71.4	19.3	3.70

[a]Conditions: monomer (1.0 mmol for $(Me)_2PL$, 3.0 mmol for $[(Me)_2PL]_3$), initiator (I) = BnOH. [b]Conversion determined by ^{1}H NMR in HFIP-d_2 or mesitylene (internal standard) in $CDCl_3$. [c]See Table 1 footnote *c* for definitions.

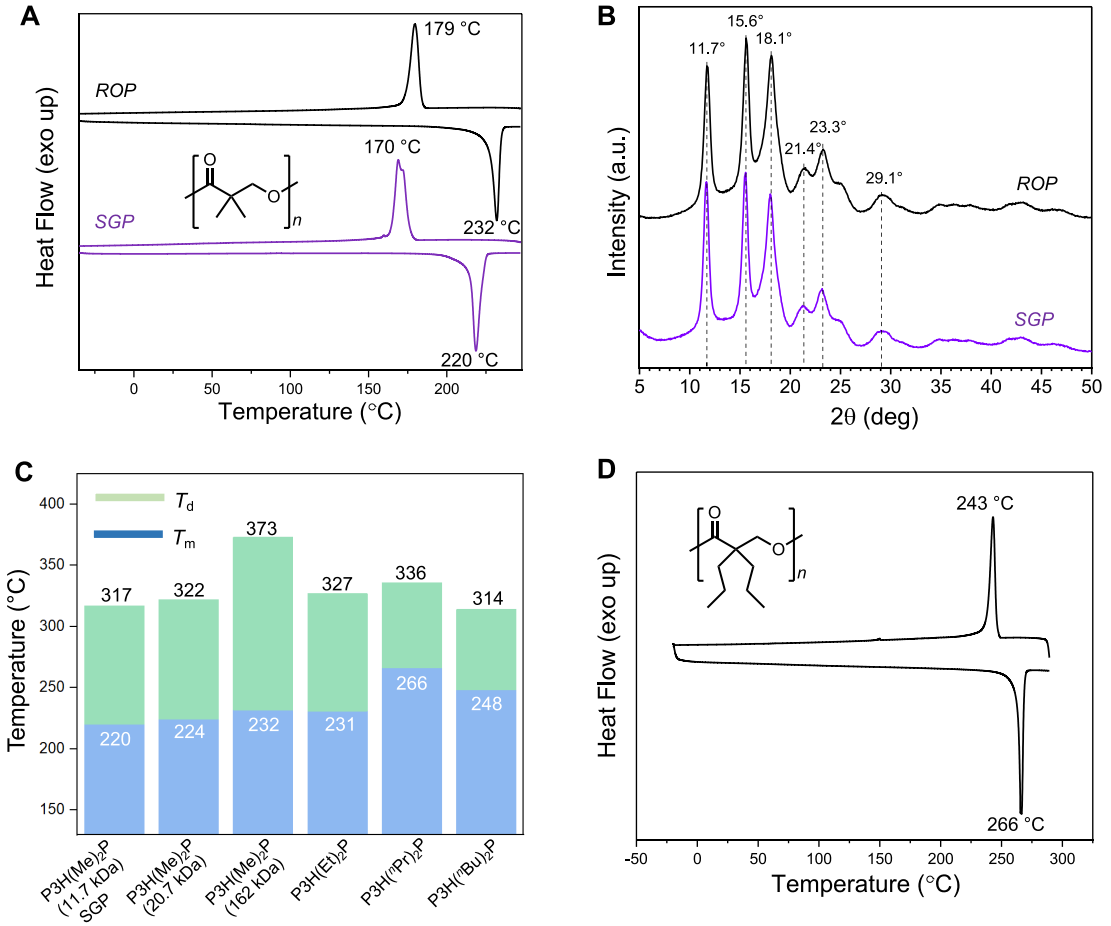

Figure 4. Thermal properties and crystallinity of $P3H(R)_2P$. (A) DSC thermograms (10 °C/min) for $P3H(Me)_2P$ (M_w = 232 kDa, M_n = 162 kDa) obtained by ROP (black) and $P3H(Me)_2P$ (M_w = 26.4 kDa, M_n = 11.7 kDa) obtained by SGP (purple). Exothermic crystallization peaks (T_c) obtained from the first cooling scan and endothermic peaks (T_m) from the second heating scan. (B) WAXS profiles of $P3H(Me)_2P$ prepared by ROP (black) and SGP (purple), showing identical diffraction patterns and peak intensities (thus the same crystal structure and the degree of crystallinity). (C) A compilation of T_m and T_d values for $P3H(Me)_2P$ obtained by SGP (M_w = 26.4 kDa, M_n = 11.7 kDa) and $P3H(R)_2P$ (R = Me, Et, ^{n}Pr, ^{n}Bu) obtained by ROP. Numbers included in the parentheses on *x*-axis are M_n values. (D) DSC thermogram (10 °C/min) for $P3H(^n Pr)_2P$: T_c = 243 °C (obtained from the first cooling scan); T_m = 266 °C (obtained from the second hearing scan); T_g = 75 °C (by DMA, Figure S24).

out in solvent-less, bulk conditions and optimized at 70 °C. Organic superbase ^{t}Bu-P_4 (1-*tert*-butyl-4,4,4-tris(dimethylamino)-2,2-bis[tris(dimethylamino)-phosphoranylidenamino]-2λ^5,4λ^5-catenadi(phosphazene)) exhibited both high polymerization activity and efficiency, affording high-molar-mass $P3H(Me)_2P$. For example, employing a $[(Me)_2PL]/[^t Bu\text{-}P_4]/[BnOH]$ ratio of 6400:1:1, the solvent-free ROP at 70 °C achieved 99% conversion in 1 h, yielding $P3H(Me)_2P$ with M_w = 232 kDa and $Đ$ = 1.43 (Table 2, Run 7). Other less basic organic catalysts such as TBD (1,5,7-triazabicyclo[4.4.0]dec-5-ene) and DBU (1,8-diazabicyclo[5.4.0]undec-7-ene) are less effective, achieving

https://doi.org/10.1021/jacs.4c11920
J. Am. Chem. Soc. 2024, 146, 29895−29904

the highest M_w of 110 kDa (Table 2, Runs 1−4). The recovered $(Me)_2PL$ was repolymerized through the ^tBu-P_4 mediated ROP ($[(Me)_2PL]:[^tBu\text{-}P_4] = 6400:1$) at 70 °C, affording P3H$(Me)_2$P with a similar M_w (M_w = 187 kDa) to that of the virgin polymer. Notably, heating ROP-P3H$(Me)_2$P (M_w = 23.0 kDa), obtained with $[(Me)_2PL]:[^tBu\text{-}P_4]:[BnOH] = 400:1:1$, mixed with 5 wt % NaOMe at 230 °C for 24 h under vacuum (∼0.2 Torr) distilled off $(Me)_2PL$ in 51% isolated yield and $[(Me)_2PL]_3$ in 35% isolated yield (Table S1, Run 7), achieving 86% total recovery of the monomer and trimer. In comparison, the depolymerization of P3H$(Me)_2$P by employing other conditions (5 wt % sodium pivalate, 306 °C, ∼ 0.1 Torr)[38] achieved a quantitative polymer conversion, but the resulting products were a mixture of $(Me)_2PL$ (21%) and $[(Me)_2PL]_3$ (2%), plus CO_2 and isobutene as the major side products.

The ROP of the 12-membered lactone $[(Me)_2PL]_3$ was also investigated. Given the lower reactivity of this trimer, we resorted to high-temperature polymerization under melt and neat conditions. With a ratio of $[(Me)_2PL]_3/[^tBu\text{-}P_4]/[BnOH]$ of 100:1:1, the ROP achieved quantitative conversion after 12 h, affording P3H$(Me)_2$P with M_w = 31.2 kDa and $Đ$ = 2.97 (Table 2, Run 8). However, increasing the ratio of $[(Me)_2PL]_3/[^tBu\text{-}P_4]/[BnOH]$ failed to produce a higher molar mass polymer. Next, the metal-based catalyst La$(OBn)_3$ was tested. Employing a $[(Me)_2PL]_3/[La(OBn)_3]$ ratio of 800:1, the ROP achieved a 62% conversion after 12 h, producing P3H$(Me)_2$P with M_w = 71.4 kDa (Table 2, Run 10). In addition, the direct repolymerization of $(Me)_2PL$ and $[(Me)_2PL]_3$ as a 3:1 mixture $\{(Me)_2PL:[(Me)_2PL]_3:[Zn]:^iPrOH = 300:100:1:1$, 160 °C, 12 h, $[Zn] = Zn(HMDS)_2 + L$, Table S2, run 26$\}$ achieved 96% and 51% conversion for $(Me)_2PL$ and $[(Me)_2PL]_3$, respectively, yielding P3H$(Me)_2$P with M_w = 36.6 kDa.

The above ROP results demonstrated that the SGP of 3H$(Me)_2$PA can be used to obtain oligomers or polymers with low to medium molar mass, which are effectively depolymerized to form the lactone $(Me)_2PL$ for rapid ROP to high-molar-mass PHAs. In the second closed loop for the recycling of P3H$(Me)_2$P, hydrolytic depolymerization of P3H$(Me)_2$P samples obtained from both ROP and SGP processes readily afforded the corresponding HA in quantitative yield (Table S3). For example, base-catalyzed hydrolysis of a ROP-produced P3H$(Me)_2$P sample (M_w = 23.0 kDa) with aq. NaOH in THF/MeOH at 80 °C for 24 h afforded pure 3H$(Me)_2$PA in 99% isolated yield (without chromatographic purification). The same condition is also efficient for depolymerization of the SGP-derived sample to pure 3H$(Me)_2$PA (Figure S13) in 99% yield. Notably, even for the high-molar-mass P3H$(Me)_2$P (M_w = 232 kDa), 3H$(Me)_2$PA can still be obtained in 99% yield (Table S3, Run 7). Additionally, a methanolysis study demonstrated that SGP-P3H$(Me)_2$P can be converted back to M3H$(Me)_2$P in 82% yield at 250 °C performed in an autoclave without a catalyst. Even the high-molar-mass P3H$(Me)_2$P (M_w = 232 kDa) allowed for the recovery of M3H$(Me)_2$P in 91% yield (Table S4). This closed-loop recycling of P3H$(Me)_2$P via the HA-PHA-HA or (HA-ester)-PHA-(HA-ester) loop is notable because of the near quantitative hydrolysis or methanolysis yield and similar thermal properties between the SGP- and ROP-produced P3H$(Me)_2$P materials (*vide infra*).

Thermal Properties and Crystallinity of P3H$(R)_2$P. Installation of the α,α-dimethyl substituents to P3HP increased the T_m from ∼80 °C for its parent P3HP to 232 °C (ΔH_f = 126 J/g) for the resulting P3H$(Me)_2$P (M_w = 232 kDa) obtained from the ROP, as shown by their differential scanning calorimetry (DSC) thermograms (Figures 4A and S16). Worth noting here is that the T_m of the P3H$(Me)_2$P produced by SGP with a much lower molar mass (M_w = 26.4 kDa) is similarly high, 220 °C, also accompanied by a high ΔH_f of 112 J/g for a high degree of crystallinity (Figures 4A and S14). Hence, SGP offers an alternative, convenient pathway to yield P3H$(Me)_2$P with comparable thermal properties. However, the T_m of the P3H$(Me)_2$P with a low molar mass of M_n = 2.22 kDa (by NMR) prepared by SGP of 3-hydroxypivalic acid using H_3PO_4 was reported to be only 106 °C.[67]

Wide angle X-ray scattering (WAXS) profiles of the ROP-produced P3H$(Me)_2$P (M_w = 232 kDa) show three major diffraction peaks centered at $2\theta \approx 11.7$, 15.6, and 18.1°, accompanied by other minor diffraction peaks of lower intensities at higher 2θ values (Figure 4B). After the background baseline and the scattering halo of the amorphous phase (obtained by heating the sample above its T_m) were subtracted from the whole diffraction profile, the degree of crystallinity (x_c) was calculated to be x_c = 76% for P3H$(Me)_2$P (Figure S17). Also noteworthy is that essentially identical WAXS profiles were observed for the P3H$(Me)_2$P samples produced from SGP and ROP (Figure 4B), indicating the same crystal structure and the degree of the crystallinity. Owing to its high crystallinity, the glass-transition temperature (T_g) of P3H$(Me)_2$P was not observable from its DSC thermogram. Alternatively, its T_g was measured to be 70 °C from the tan δ peak maxima by dynamic mechanical analysis (DMA, Figure S23).

Other dialkyl-substituted PHAs, P3H$(R)_2$P (R = Et, ^{n}Pr, ^{n}Bu), were readily synthesized via the ROP of their corresponding lactones (Table S2). The thermal properties of these PHAs samples were analyzed by DSC and thermogravimetric analysis (TGA) and then compared. Impressively, the decomposition temperature (T_d, the temperature at 5% weight loss) of P3H$(Me)_2$P (M_w = 232 kDa) reached to 373 °C, with a T_{max} (maximum decomposition temperature) of 435 °C,[28] highlighting the much-enhanced thermal stability compared to a typical T_d value of 250 °C for PHAs without the α,α-disubstitution such as P3HP and P3HB.

Effects of the alkyl chain length in P3H$(R)_2$P on their T_m and T_d values have been examined, and the results are summarized in Figure 4C. Three interesting trends in the effects of different substituents are noteworthy. First, there is an increase in T_m for P3H$(R)_2$P with increasing the chain length of the dialkyl groups form Me to Et and eventually to ^{n}Pr, leading to the highest T_m of 266 °C (Figure 4D, T_g = 75 °C, Figure S24) for P3H$(^nPr)_2$P (Figures S18−22). To the best of our knowledge, this T_m values represents the highest T_m within the PHA family. Further increasing the T_m of PHAs to reach that of PET and nylons ($T_m \geq 250$ °C) typically used in the textile industry would expand their potential use in high-temperature applications, such as PHA fibers as PET and nylon alternatives for textiles. The differences in T_m values with changing alkyl substituents in P3H$(R)_2$P are likely due to the crystallization of different crystal structures. The increase in T_m with R going from Me to Et to ^{n}Pr may be indicative of a more efficient and denser crystal packing achieved with longer substituents. The study and analysis of the crystal structures of P3H$(R)_2$P with different R substituents will be reported elsewhere. Second, all of the P3H$(R)_2$P displayed excellent thermal stability with T_d generally >310 to 373 °C (Figures 4C and S25−31). Third, the molar mass has a significant effect on the T_d of P3H$(Me)_2$P, but it hardly affects T_m. For example, when the M_w of P3H$(Me)_2$P prepared by ROP was increased from 23.0 to 232 kDa, the T_d was enhanced by 51

https://doi.org/10.1021/jacs.4c11920
J. Am. Chem. Soc. 2024, 146, 29895−29904

°C from 322 to 373 °C, but the T_m was changed only slightly (by 8 °C).

Mechanical and Rheological Properties of P3H(R)$_2$P. Owing to their fast crystallization and high degree of crystallinity, the α,α-dialkylated derivatives P3H(Me)$_2$P (M_w = 232 kDa), P3H(Et)$_2$P (M_w = 99.6 kDa), and P3H(^{n}Pr)$_2$P (unknown M_w due to its insolubility in SEC solvents, even in HFIP) are highly brittle, with a low ε_b value <5% (Figures 5A and S34). However, this mechanical brittleness can be overcome by forming a Me/Et (50/50) or Me/^{n}Pr (50/50) random copolymers, P3H(Me/Et)$_2$P and P3H(Me/^{n}Pr)$_2$P (Table S2, Runs 18, 20, Figures S35 and S36). These copolymers maintain high T_m values (216, 251 °C, Figures S19 and S21). More significantly, the semicrystalline PHA copolymer P3H(Me/Et)$_2$P is ductile and tough with ultimate tensile strength (σ) = 38.2 ± 2.0 MPa, elastic modulus (E) = 720 ± 30 MPa, and ε_b = 335 ± 8% (Figures 5A and S37, Table S6). Furthermore, with incorporation of more flexible di(n-propyl) groups, copolymer P3H(Me/^{n}Pr)$_2$P exhibits further enhanced ductility with ε_b = 434 ± 46%, while maintaining a good modulus of E = 460 ± 20 MPa (Figures 5A and S38, Table S7). We also tested the mechanical recyclability of copolymer P3H(Me/^{n}Pr)$_2$P through repeated melt-processing. After five cycles, the tensile properties did not change significantly (Figure S39), confirming the thermal stability and mechanical recyclability of the copolymer under repeated processing conditions.

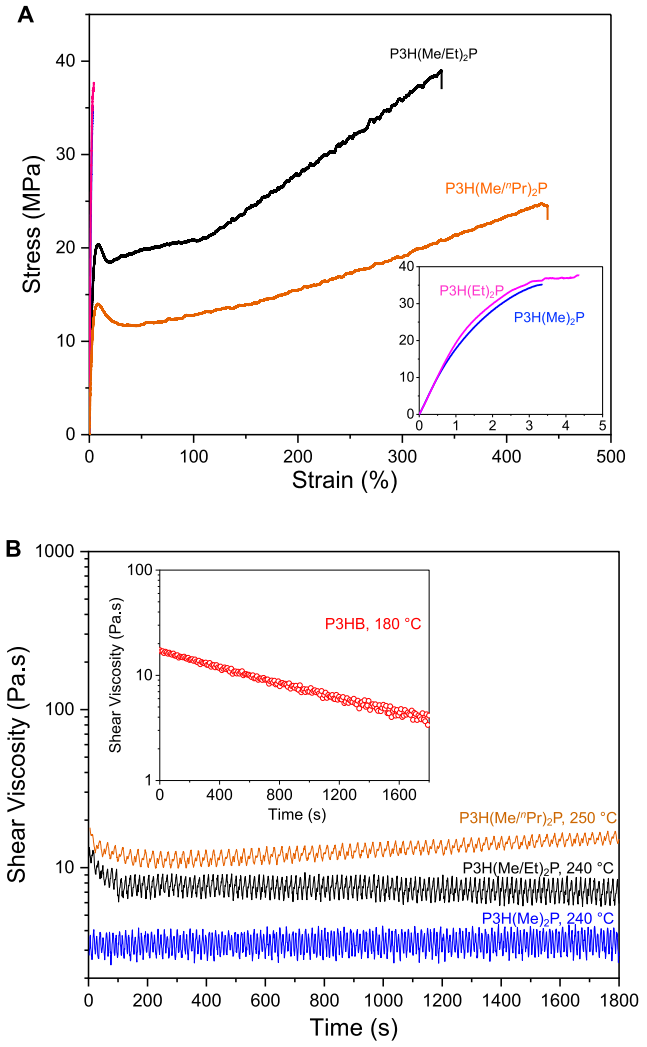

Figure 5. Mechanical and rheological properties of P3H(R)$_2$P. (A) Representative stress−strain curves of P3H(Me)$_2$P (M_w = 232 kDa, blue), P3H(Et)$_2$P (M_w = 99.6 kDa, pink), P3H(Me/Et)$_2$P (M_w = 82.4 kDa, black), and P3H(Me/^{n}Pr)$_2$P (orange). (B) Overlays of shear viscosity in the melt (shear rate $\dot{\gamma}$ = 1 s^{-1}): P3HB (M_w = 118 kDa, red), P3H(Me)$_2$P (M_w = 117 kDa, blue), P3H(Me/Et)$_2$P (M_w = 99.6 kDa, black), and P3H(Me/^{n}Pr)$_2$P (orange).

To examine the melt processability of P3H(R)$_2$P, we monitored the shear viscosity change over a period of 30 min for P3H(Me)$_2$P, P3H(Me/Et)$_2$P, and P3H(Me/^{n}Pr)$_2$P at temperatures above their T_m values in a continuous flow mode at a shear rate of 1 s^{-1} (Figure 5B). A reference sample, *it*-P3HB (M_w = 118 kDa, T_m = 170 °C), was also subjected to the same shear viscosity test in melt (180 °C), which showed a 76% decrease in its shear viscosity after 30 min.[28] In sharp contrast, as shown in Figure 5B, the shear viscosities for all of the P3H(R)$_2$P samples, P3H(Me)$_2$P, P3H(Me/Et)$_2$P, and P3H(Me/^{n}Pr)$_2$P, remained constant without obvious decrease over 30 min at 240 or 250 °C, which are well above their corresponding melting temperature. Overall, the studies in shear viscosity presented here consolidate the effectiveness of the strategy of removing the α-protons from the PHA repeating units for enhancing their thermal stability and enabling their melt processability.

On the other hand, in the presence of a base catalyst, the high-T_m P3H(^{n}Pr)$_2$P obtained through ROP can be effectively depolymerized at 245 °C (below its T_m) with 5 wt % NaOH, recovering a 70% yield of (^{n}Pr)$_2$PL (Table S5, Figure S40). Notably, in contrast to the depolymerization of P3H(Me)$_2$P, no trimeric [(^{n}Pr)$_2$PL]$_3$ was observed during the depolymerization of P3H(^{n}Pr)$_2$P. This differing depolymerization behavior is ascribed to the significantly larger steric hindrance in the possible [(^{n}Pr)$_2$PL]$_3$ than that in [(Me)$_2$PL]$_3$, as indicated by computational simulations (Figure S41). Additionally, the copolymer P3H(Me/^{n}Pr)$_2$P can also be effectively depolymerized under the current standard conditions, yielding (Me)$_2$PL and (^{n}Pr)$_2$PL in a 1:1 ratio with a 67% isolated yield (Figure S42).

Barrier Properties. Barriers of P3H(Me)$_2$P (M_w = 232 kDa) and P3H(Me/Et)$_2$P (M_w = 82.4 kDa) toward permeation of water vapor and oxygen have been investigated, compared to representative commercially available barrier polymers, and are summarized in Figure 6 (Tables S8 and S9). Both homopolymer P3H(Me)$_2$P and copolymer P3H(Me/Et)$_2$P showed a good barrier to water vapor, with a relatively low water vapor transmission rate (WVTR) of 2.72 ± 0.71 and 2.35 ± 0.25 g·mm·m^{-2}·day^{-1}, respectively. These values are significantly lower than biodegradable poly(L-lactide) (PLLA) (5.7 ± 0.50 g·mm·m^{-2}·day^{-1}) and poly(butylene adipate-*co*-terephthalate) (PBAT) (12.76 ± 0.34 g·mm·m^{-2}·day^{-1}) (Figure 6A). However, the WVTR of these two P3H(R)$_2$P samples is somewhat higher than that of PET, low-density polyethylene (LDPE), and pure *it*-P3HB.

Regarding oxygen permeability (PO_2), P3H(Me)$_2$P displayed an impressively low value of only 0.058 ± 0.007 Barrer, which is much lower than that of LDPE (5.42 ± 0.18 Barrer), PLLA (0.26 ± 0.01 Barrer), and PBAT (0.89 ± 0.01 Barrer) and even lower than that of PET (0.09 ± 0.0 Barrer). The PO_2 value of copolymer P3H(Me/Et)$_2$P (0.16 ± 0.0002 Barrer) is somewhat higher than that of P3H(Me)$_2$P, but it is still considerably lower than that of LDPE, PLLA, and PBAT (Figure 6B). On the other hand, *it*-P3HB exhibited the lowest PO_2 value of 0.01 ± 0.003 in this series of barrier polymers investigated.

https://doi.org/10.1021/jacs.4c11920
J. Am. Chem. Soc. 2024, 146, 29895−29904

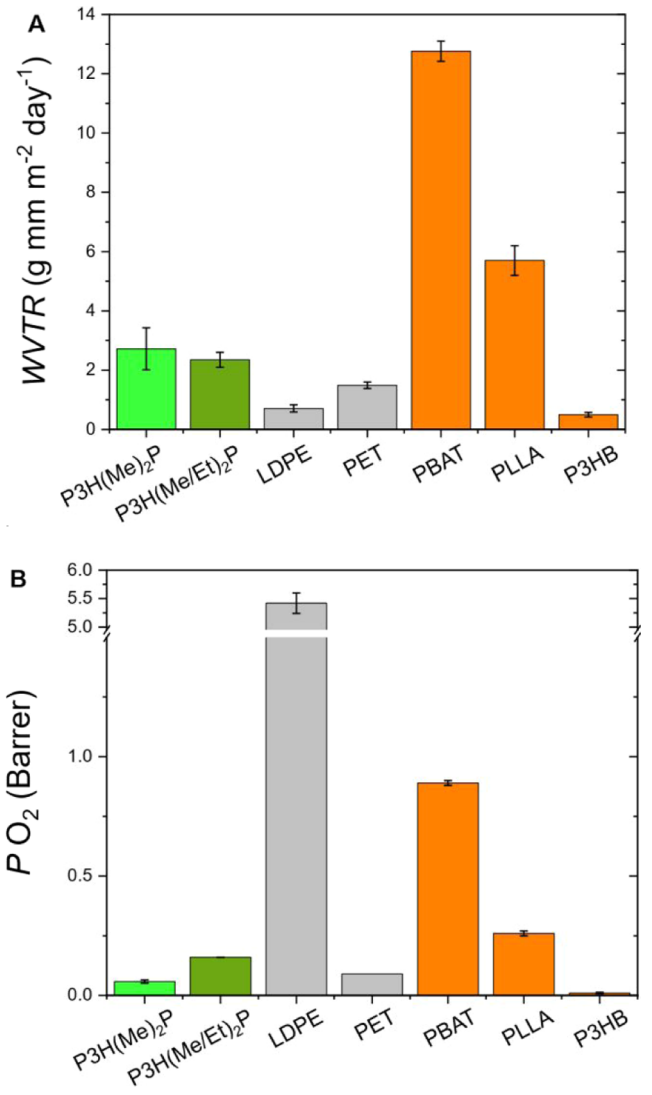

Figure 6. Barrier properties of two representative P3H(R)$_2$P samples, compared with commercially available barrier polymers LDPE, PET, PBAT, PLLA, and P3HB. (A) Water vapor transmission rate (WVTR) of P3H(Me)$_2$P and P3H(Me/Et)$_2$P. (B) Oxygen permeability coefficient (PO_2) of P3H(Me)$_2$P and P3H(Me/Et)$_2$P. The error bars correspond to the s.d. of at least five (WVTR) or at least two (PO_2) replicates.

Overall, P3H(R)$_2$P showed significantly better water vapor and oxygen gas barrier properties than did PLLA, PBAT, and LDPE (PO_2). Although P3H(R)$_2$P samples displayed somewhat higher permeability than *it*-P3HB, they exhibit balanced mechanical and transport properties, which make them interesting candidates for packaging applications. Particularly, P3H(R)$_2$P offers similar or even higher oxygen barriers relative to commercial barrier polymers LDPE and PET, highlighting potential as a more sustainable alternative to LDPE and PET.

CONCLUSIONS

In summary, despite extensive research on the high-T_m and highly crystalline P3H(Me)$_2$P, an efficient synthetic method to this PHA with low to high molar mass, overcoming the extreme brittleness and closed-loop chemical recycling, remained elusive until this report. This work not only solved the aforementioned three challenges but also led to a new PHA with record-high T_m. Four key results are noteworthy. First, the convenient SGP of the HA, 3H(Me)$_2$PA, and its methyl ester, M3H(Me)$_2$P, afforded P3H(Me)$_2$P with low to medium molar mass but still high T_m and crystallinity, while the efficient ROP of the lactone monomer (Me)$_2$PL led to P3H(Me)$_2$P with high molar mass (M_w = 232 kDa) and higher T_m (232 °C). The successful application of SGP in P3H(Me)$_2$P synthesis is attributed to the absence of α-hydrogens, which suppresses the side reactions, and the presence of a primary alcohol in the HA, which ensures sufficient reactivity. Second, through formation of PHA copolymers P3H(Me/R)$_2$P (R = Et, ^{n}Pr), PHAs with both high tensile strength and ductility (thus toughness), coupled with high barriers to water vapor and oxygen (superior to commercial LDPE, PLLA, and PBAT), have been created. Third, base-catalyzed depolymerization of P3H(Me)$_2$P-CO_2Me, obtained from SGP of M3H(Me)$_2$P, yields the desired 4-membered lactone monomer (Me)$_2$PL as the major product, while the depolymerization of P3H(Me)$_2$P-CO_2H, obtained from SGP of 3H(Me)$_2$PA, affords the 12-membered lactone trimer [(Me)$_2$PL]$_3$ as the major product. Both lactones can be repolymerized back to the PHA, closing the ROP loop, while hydrolytic depolymerization to the HA closes the SGP loop. Fourth, the PHA structure/property study led to P3H(^{n}Pr)$_2$P with an exceptionally high T_m of 266 °C which, to the best of our knowledge, represents the highest T_m value reported for the PHA family.

ASSOCIATED CONTENT

Supporting Information

The Supporting Information is available free of charge at https://pubs.acs.org/doi/10.1021/jacs.4c11920.

Experimental and DFT details; additional figures (Figures S1−S42) and tables (Tables S1−S10); and characterization data (PDF)

Accession Codes

CCDC 2314002 contains the supplementary crystallographic data for this paper. These data can be obtained free of charge via www.ccdc.cam.ac.uk/data_request/cif or by emailing data_request@ccdc.cam.ac.uk or by contacting The Cambridge Crystallographic Data Centre, 12 Union Road, Cambridge CB2 1EZ, U.K.; fax: +44 1223 336033.

AUTHOR INFORMATION

Corresponding Author

Eugene Y.-X. Chen − *Department of Chemistry, Colorado State University, Fort Collins, Colorado 80523-1872, United States;* orcid.org/0000-0001-7512-3484; Email: eugene.chen@colostate.edu

Authors

Li Zhou − *Department of Chemistry, Colorado State University, Fort Collins, Colorado 80523-1872, United States;* orcid.org/0000-0001-9607-3877

Zhen Zhang − *Department of Chemistry, Colorado State University, Fort Collins, Colorado 80523-1872, United States*

Ainara Sangroniz − *Department of Chemistry, Colorado State University, Fort Collins, Colorado 80523-1872, United States; POLYMAT and Department of Polymers and Advanced Materials: Physics, Chemistry and Technology, Faculty of Chemistry, University of the Basque Country UPV/EHU, 20018 Donostia-San Sebastián, Spain*

Changxia Shi − *Department of Chemistry, Colorado State University, Fort Collins, Colorado 80523-1872, United States*

Ravikumar R. Gowda − *Department of Chemistry, Colorado State University, Fort Collins, Colorado 80523-1872, United States*

Miriam Scoti − *Department of Chemistry, Colorado State University, Fort Collins, Colorado 80523-1872, United States; Dipartimento di Scienze Chimiche, Università di Napoli Federico II, 80126 Napoli, Italy;* orcid.org/0000-0001-9225-1509

Deepak K. Barange − *Department of Chemistry, Colorado State University, Fort Collins, Colorado 80523-1872, United States*

Clarissa Lincoln − *Renewable Resources and Enabling Sciences Center, National Renewable Energy Laboratory, Golden, Colorado 80401, United States; BOTTLE Consortium, Golden, Colorado 80401, United States*

Gregg T. Beckham − *Renewable Resources and Enabling Sciences Center, National Renewable Energy Laboratory, Golden, Colorado 80401, United States; BOTTLE Consortium, Golden, Colorado 80401, United States;* orcid.org/0000-0002-3480-212X

Complete contact information is available at: https://pubs.acs.org/10.1021/jacs.4c11920

Notes

The authors declare the following competing financial interest(s): E.Y.-X.C. and L.Z. are named inventors on a pending PCT/US patent application (2023/021512) based on provisions US2022 63/340.168 and 63/434.550, submitted by Colorado State University Research Foundation, which covers chemically circular PHAs. The other authors declare no competing interests.

■ ACKNOWLEDGMENTS

Funding was provided by the U.S. Department of Energy, Office of Energy Efficiency and Renewable Energy, Advanced Materials and Manufacturing Technologies Office (AMMTO), and Bioenergy Technologies Office (BETO). This work was performed as part of the Bio-Optimized Technologies to keep Thermoplastics out of Landfills and the Environment (BOTTLE) Consortium and was supported by AMMTO and BETO under Contract DE-AC36-08GO28308 with the National Renewable Energy Laboratory (NREL), operated by Alliance for Sustainable Energy, LLC. The BOTTLE Consortium includes members from Colorado State University. In the early stage of the PHA project, the work was supported by the U.S. National Science Foundation (NSF-1955482 to EYC) and Basque Country Government (GC IT 1667-22 to AS).

■ REFERENCES

(1) Müller, H.; Seebach, D. Poly(hydroxyalkanoates): A Fifth Class of Physiologically Important Organic Biopolymers? *Angew. Chem., Int. Ed.* **1993**, *32*, 477−502.

(2) Sudesh, K.; Abe, H.; Doi, Y. Synthesis, structure and properties of polyhydroxyalkanoates: biological polyesters. *Prog. Polym. Sci.* **2000**, *25*, 1503−1555.

(3) Lenz, R. W.; Marchessault, R. H. Bacterial polyesters: biosynthesis, biodegradable plastics and biotechnology. *Biomacromolecules* **2005**, *6*, 1−8.

(4) Chen, G. Q. A microbial polyhydroxyalkanoates (PHA) based bio- and materials industry. *Chem. Soc. Rev.* **2009**, *38*, 2434−2446.

(5) Laycock, B.; Halley, P.; Pratt, S.; Werker, A.; Lant, P. The chemomechanical properties of microbial polyhydroxyalkanoates. *Prog. Polym. Sci.* **2013**, *38*, 536−583.

(6) Afzal, M.; Hameed, S. Bacterial polyhydroxyalkanoates-eco-friendly next generation plastic: Production, biocompatibility, biodegradation, physical properties and applications. *Green Chem. Lett. Rev.* **2015**, *8*, 56−77.

(7) Anjum, A.; Zuber, M.; Zia, K. M.; Noreen, A.; Anjum, M. N.; Tabasum, S. Microbial production of polyhydroxyalkanoates (PHAs) and its copolymers: A review of recent advancements. *Int. J. Biol. Macromol.* **2016**, *89*, 161−174.

(8) Taguchi, S.; Iwata, T.; Abe, H.; Doi, Y. Poly(hydroxyalkanoate)s. In *Polymer Science: A Comprehensive Reference*; Matyjaszewski, K.; Möller, M., Eds.; Elsevier: Amsterdam, 2012; pp 157−182.

(9) Raza, Z. A.; Abid, S.; Banat, I. M. Polyhydroxyalkanoates: Characteristics, production, recent developments and applications. *Int. Biodeterior. Biodegrad.* **2018**, *126*, 45−56.

(10) Bedade, D. K.; Edson, C. B.; Gross, R. A. Emergent Approaches to Efficient and Sustainable Polyhydroxyalkanoate Production. *Molecules* **2021**, *26*, 3463.

(11) Tan, D.; Wang, Y.; Tong, Y.; Chen, G. Q. Grand Challenges for Industrializing Polyhydroxyalkanoates (PHAs). *Trends Biotechnol.* **2021**, *39*, 953−963.

(12) Li, H.; Shakaroun, R. M.; Guillaume, S. M.; Carpentier, J. F. Recent Advances in Metal-Mediated Stereoselective Ring-Opening Polymerization of Functional Cyclic Esters towards Well-Defined Poly(hydroxy acid)s: From Stereoselectivity to Sequence-Control. *Chem. - Eur. J.* **2020**, *26*, 128−138.

(13) Westlie, A. H.; Quinn, E. C.; Parker, C. R.; Chen, E. Y.-X. Synthetic biodegradable polyhydroxyalkanoates (PHAs): Recent advances and future challenges. *Prog. Polym. Sci.* **2022**, *134*, No. 101608.

(14) Tang, X.; Chen, E. Y.-X. Toward Infinitely Recyclable Plastics Derived from Renewable Cyclic Esters. *Chem* **2019**, *5*, 284−312.

(15) Shi, C.; Quinn, E. C.; Diment, W. T.; Chen, E. Y.-X. Recyclable and (Bio)degradable Polyesters in a Circular Plastics Economy. *Chem. Rev.* **2024**, *124*, 4393−4478.

(16) Adamus, G.; Dominski, A.; Kowalczuk, M.; Kurcok, P.; Radecka, I. From Anionic Ring-Opening Polymerization of β-Butyrolactone to Biodegradable Poly(hydroxyalkanoate)s: Our Contributions in This Field. *Polymers* **2021**, *13*, No. 4365.

(17) Kramer, J. W.; Treitler, D. S.; Dunn, E. W.; Castro, P. M.; Roisnel, T.; Thomas, C. M.; Coates, G. W. Polymerization of enantiopure monomers using syndiospecific catalysts: a new approach to sequence control in polymer synthesis. *J. Am. Chem. Soc.* **2009**, *131*, 16042−16044.

(18) Bruckmoser, J.; Pongratz, S.; Stieglitz, L.; Rieger, B. Highly Isoselective Ring-Opening Polymerization of rac-beta-Butyrolactone: Access to Synthetic Poly(3-hydroxybutyrate) with Polyolefin-like Material Properties. *J. Am. Chem. Soc.* **2023**, *145*, 11494−11498.

(19) Huang, H.-Y.; Xiong, W.; Huang, Y.-T.; Li, K.; Cai, Z.; Zhu, J.-B. Spiro-salen catalysts enable the chemical synthesis of stereoregular polyhydroxyalkanoates. *Nat. Catal.* **2023**, *6*, 720−728.

(20) Quinn, E. C.; Westlie, A. H.; Sangroniz, A.; Caputo, M. R.; Xu, S.; Zhang, Z.; Urgun-Demirtas, M.; Muller, A. J.; Chen, E. Y.-X. Installing Controlled Stereo-Defects Yields Semicrystalline and Biodegradable Poly(3-Hydroxybutyrate) with High Toughness and Optical Clarity. *J. Am. Chem. Soc.* **2023**, *145*, 5795−5802.

(21) Zhang, Z.; Quinn, E. C.; Olmedo-Martinez, J. L.; Caputo, M. R.; Franklin, K. A.; Muller, A. J.; Chen, E. Y.-X. Toughening Brittle Bio-P3HB with Synthetic P3HB of Engineered Stereomicrostructures. *Angew. Chem., Int. Ed.* **2023**, *62*, No. e202311264.

(22) Chellali, J. E.; Woodside, A. J.; Yu, Z.; Neogi, S.; Külaots, I.; Guduru, P. R.; Robinson, J. R. Access to Stereoblock Polyesters via Irreversible Chain-Transfer Ring-Opening Polymerization (ICT-ROP). *J. Am. Chem. Soc.* **2024**, *146*, 11562−11569.

(23) Yang, J.-C.; Yang, J.; Li, W.-B.; Lu, X.-B.; Liu, Y. Carbonylative Polymerization of Epoxides Mediated by Tri-metallic Complexes: A Dual Catalysis Strategy for Synthesis of Biodegradable Polyhydroxyalkanoates. *Angew. Chem., Int. Ed.* **2022**, *61*, No. e202116208.

(24) Amgoune, A.; Thomas, C. M.; Ilinca, S.; Roisnel, T.; Carpentier, J.-F. Highly Active, Productive, and Syndiospecific Yttrium Initiators for the Polymeriation of Racemic β-Butyrolactone. *Angew. Chem., Int. Ed.* **2006**, *45*, 2782−2784.

(25) Furutate, S.; Kamoi, J.; Nomura, C. T.; Taguchi, S.; Abe, H.; Tsuge, T. Superior thermal stability and fast crystallization behavior of a novel, biodegradable a-methylated bacterial polyester. *NPG Asia Mater.* **2021**, *13*, No. 31.
(26) Zhou, Z.; LaPointe, A. M.; Shaffer, T. D.; Coates, G. W. Nature-inspired methylated polyhydroxybutyrates from C1 and C4 feedstocks. *Nat. Chem.* **2023**, *15*, 856−861.
(27) Zhou, Z.; LaPointe, A. M.; Coates, G. W. Atactic, Isotactic, and Syndiotactic Methylated Polyhydroxybutyrates: An Unexpected Series of Isomorphic Polymers. *J. Am. Chem. Soc.* **2023**, *145*, 25983−25988.
(28) Zhou, L.; Zhang, Z.; Shi, C.; Scoti, M.; Barange, D. K.; Gowda, R. R.; Chen, E. Y.-X. Chemically circular, mechanically tough, and melt-processable polyhydroxyalkanoates. *Science* **2023**, *380*, 64−69.
(29) Scoti, M.; Zhou, L.; Chen, E. Y.-X.; Rosa, C. D. Crystal Structure of Atactic and Isotactic Poly(3-hydroxy-2,2-dimethylbutyrate): A Chemically Recyclable Poly(hydroxyalkanoate) with Tacticity-Independent Crystallinity. *Macromolecules* **2024**, *57*, 4357−4373.
(30) Bossion, A.; Heifferon, K. V.; Meabe, L.; Zivic, N.; Taton, D.; Hedrick, J. L.; Long, T. E.; Sardon, H. Opportunities for organocatalysis in polymer synthesis via step-growth methods. *Prog. Polym. Sci.* **2019**, *90*, 164−210.
(31) Kricheldorf, H. *Polycondensation*; Springer: Berlin, 2014.
(32) Mayne, N. R. The polymerization of pivalolactone. *Chem. Technol.* **1972**, *2*, 728−733.
(33) Morimoto, K.; Tanaka, Y.; Tanaka, T.; Okubo, T. Poly-pivalolactone with high m.p., good hydrolysis resistance, and thermal stability, and manufacture therefor. Japanese Patent JP 163779; 2013.
(34) Hall, H. K. The Nucleophile-Initiated Polymerization of α,α-Disubstituted β-Lactones. *Macromolecules* **1969**, *2*, 488−497.
(35) Meille, S. V.; Konishi, T.; Geil, P. H. Morphology of polypivalolactone: A polymer with a direction. *Polymer* **1984**, *25*, 773−777.
(36) Perego, G.; Melis, A.; Cesari, M. The crystal structure of polypivalolactone. *Makromol. Chem.* **1972**, *157*, 269−278.
(37) Zhu, B.; He, Y.; Asakawa, N.; Yoshie, N.; Nishida, H.; Inoue, Y. A New Crystal Form, Polymorphism, and Multi-Morphology in Biodegradable Poly(3-hydroxypropionate). *Macromol. Rapid Commun.* **2005**, *26*, 581−585.
(38) Van der Ven, S.; Binsergen, F. L. Process for recovery of pivalolactone from polymers thereof. U.S. Patent US 3751435; 1973.
(39) Wiley, R. H. Mass Spectral Characteristics of Pivalolactones and Polypivalolactone. *J. Macromol. Sci., Chem.* **1970**, *A4*, 1797−1818.
(40) Kricheldorf, H. R.; Lüderwald, I. Strukturuntersuchung von polyestern durch direkten abbau im massenspektrometer, 3. Poly-b-propiolacton, poly-b-pivalolacton und poly-d-valerolacton. *Makromol. Chem.* **1978**, *179*, 421−427.
(41) Lüderwald, I.; Sauer, W. Über den thermischen Abbau des Polypivalolactons in cyclische Oligomere. *Makromol. Chem.* **1981**, *182*, 861−865.
(42) Garozzo, D.; Giuffrida, M.; Montaudo, G. Primary thermal decomposition processes in aliphatic polyesters investigated by chemical ionization mass spectrometry. *Macromolecules* **1986**, *19*, 1643−1649.
(43) Montaudo, G. Mass spectral determination of cyclic oligomer distributions in polymerization and degradation reactions. *Macromolecules* **1991**, *24*, 5829−5833.
(44) Manring, L. E.; Blume, R. C.; Dee, G. T. Thermal degradation of poly(2,2-dialkyl-3-hydroxypropionic acid). 1. Living depolymerization. *Macromolecules* **1990**, *23*, 1902−1907.
(45) Manring, L. E.; Blume, R. C.; Simonsick, W. J.; Adelman, D. J. Thermal degradation of poly(2,2-dialkyl-3-hydroxypropionic acid). 2. Thermal degradation initiated by random scission. *Macromolecules* **1992**, *25*, 4863−4870.
(46) Matuszowicz, A.; Jedliński, Z. Synthesis of macrocyclic oligomers of pivalolactones. Crystal structure and properties of tetrolide. *J. Org. Chem.* **1995**, *60*, 6826−6828.
(47) Iliev, B.; Linden, A.; Heimgartner, H. An unexpected formation of a 14-membered cyclodepsipeptide. *Helv. Chim. Acta* **2003**, *86*, 3215−3234.
(48) Hyatt, J. A.; Raynolds, P. W. *Ketene Cycloadditions. Organic Reactions Source*; John Wiley & Sons, 1994.
(49) Coates, G. W.; Hubbell, A. K. Systerms and methods for regioselective carbonylation of 2,2-disubstituted epoxides. International Patent 086454; 2020.
(50) Hubbell, A. K.; Lamb, J. R.; Klimovica, K.; Mulzer, M.; Shaffer, T. D.; MacMillan, S. N.; Coates, G. W. Catalyst-Controlled Regioselective Carbonylation of Isobutylene Oxide to Pivalolactone. *ACS Catal.* **2020**, *10*, 12537−12543.
(51) Hong, M.; Chen, E. Y.-X. Chemically recyclable polymers: a circular economy approach to sustainability. *Green Chem.* **2017**, *19*, 3692−3706.
(52) Zhu, J. B.; Watson, E. M.; Tang, J.; Chen, E. Y.-X. A synthetic polymer system with repeatable chemical recyclability. *Science* **2018**, *360*, 398−403.
(53) Coates, G. W.; Getzler, Y. D. Y. L. Chemical recycling to monomer for an ideal, circular polymer economy. *Nat. Rev. Mater.* **2020**, *5*, 501−516.
(54) Abel, B. A.; Snyder, R. L.; Coates, G. W. Chemically recyclable thermoplastics from reversible-deactivation polymerization of cyclic acetals. *Science* **2021**, *373*, 783−789.
(55) Häußler, M.; Eck, M.; Rothauer, D.; Mecking, S. Closed-loop recycling of polyethylene-like materials. *Nature* **2021**, *590*, 423−427.
(56) Jehanno, C.; Alty, J. W.; Roosen, M.; De Meester, S.; Dove, A. P.; Chen, E. Y.-X.; Leibfarth, F. A.; Sardon, H. Critical advances and future opportunities in upcycling commodity polymers. *Nature* **2022**, *603*, 803−814.
(57) Ellis, L. D.; Rorrer, N. A.; Sullivan, K. P.; Otto, M.; McGeehan, J. E.; Román-Leshkov, Y.; Wierckx, N.; Beckham, G. T. Chemical and Biological Catalysis for Plastics Recycling and Upcycling. *Nat. Catal.* **2021**, *4*, 539−556.
(58) Kobayashi, T.; Hori, Y.; Kakimoto, Ma.; Imai, Y. Synthesis of biodegradable polyesters by polycondensation of methyl (R)-3-hydroxybutyrate and methyl (R)-3-hydroxy-valerate. *Makromol. Chem., Rapid Commun.* **1993**, *14*, 785−790.
(59) Lengweiler, U. D.; Fritz, M. G.; Seebach, D. Synthese monodisperser linearer und cyclischer Oligomere der (R)-3-Hydroxybuttersäure mit bis zu 128 Einheiten. *Helv. Chim. Acta* **1996**, *79*, 670−701.
(60) Melchiors, M.; Keul, H.; Höcker, H. Depolymerization of Poly[(R)-3-hydroxybutyrate] to Cyclic Oligomers and Polymerization of the Cyclic Trimer: An Example of Thermodynamic Recycling. *Macromolecules* **1996**, *29*, 6442−6451.
(61) Seebach, D.; Müller, H. M.; Bürger, H. M.; Plattner, D. A. The Triolide of (R)-3-Hydroxybutyric acid—Direct Preparation from Polyhydroxybutyrate and Formation of a Crown Estercarbonyl Complex with Na Ions. *Angew. Chem., Int. Ed.* **1992**, *31*, 434−435.
(62) Jung, M. E.; Piizzi, G. gem-disubstituent effect: theoretical basis and synthetic applications. *Chem. Rev.* **2005**, *105*, 1735−1766.
(63) Bachrach, S. M. The gem-dimethyl effect revisited. *J. Org. Chem.* **2008**, *73*, 2466−2468.
(64) Xiong, W.; Chang, W.; Shi, D.; Yang, L.; Tian, Z.; Wang, H.; Zhang, Z.; Zhou, X.; Chen, E.-Q.; Lu, H. Geminal Dimethyl Substitution Enables Controlled Polymerization of Penicillamine-Derived β-Thiolactones and Reversed Depolymerization. *Chem* **2020**, *6*, 1831−1843.
(65) Zhou, J.; Sathe, D.; Wang, J. Understanding the Structure-Polymerization Thermodynamics Relationships of Fused-Ring Cyclooctenes for Developing Chemically Recyclable Polymers. *J. Am. Chem. Soc.* **2022**, *144*, 928−934.
(66) Li, X. L.; Clarke, R. W.; Jiang, J. Y.; Xu, T. Q.; Chen, E. Y.-X. A circular polyester platform based on simple gem-disubstituted valerolactones. *Nat. Chem.* **2023**, *15*, 278−285.
(67) Prather, K. L. J.; Plata, D.; Olsen, B. D.; Joo, W.; Av-Ron, S.; Bannister, K. R.; Tantawi, O. Biodegradable sustainable polyesters and synthesizing copolymer. International Patent 081515; 2023.

https://doi.org/10.1021/jacs.4c11920
J. Am. Chem. Soc. 2024, 146, 29895−29904